Sivakumar, V. *et al.* (2015). *Géotechnique* **65**, No. 2, 111–125 [http://dx.doi.org/10.1680/geot.14.P.019]

Wetting of compacted clays under laterally restrained conditions: initial state, overburden pressure and mineralogy

V. SIVAKUMAR*, J. ZAINI†, D. GALLIPOLI‡ and B. SOLAN§

Compacted clay fills are generally placed at the optimum value of water content and, immediately after placement, they are unsaturated. Wetting might subsequently occur due, for example, to rainfall infiltration, which can cause volumetric deformation of the fill (either swell or collapse) with associated loss of shear strength and structural integrity. If swelling takes place under partially restrained deformation, due for example to the presence of a buried rigid structure or a retaining wall, additional stresses will develop in the soil and these can be detrimental to the stability of walling elements and other building assets. Factors such as dry density, overburden pressure, compaction water content and type of clay are known to influence the development of stresses. This paper investigates these factors by means of an advanced stress path testing programme performed on four different clays with different mineralogy, index properties and geological histories. Specimens of kaolin clay, London Clay, Belfast Clay and Ampthill Clay were prepared at different initial states and subjected to 'controlled' wetting, whereby the suction was reduced gradually to zero under laterally restrained conditions (i.e. K_0 conditions). The results showed that the magnitude of the increase in horizontal stresses (and therefore the increase of K_0) is influenced by the overburden pressure, compaction water content, dry density at the time of compaction and mineralogy.

KEYWORDS: clays; retaining walls; stress paths; suction

INTRODUCTION

Compacted clay fills are usually placed at about the optimum water content (OWC) as measured from standard Proctor compaction tests. The objective is to attain the maximum dry density (MDD) corresponding to Proctor compaction, although the compaction procedures used in the field might differ from the Proctor standard. Immediately after construction, clay fills are unsaturated and, during subsequent wetting, they undergo volumetric deformation and loss of shear strength, which can in turn lead to surface settlement or heave, and even collapse or failure at saturation (Alonso *et al.*, 1990; Clayton *et al.*, 1991; Charles, 1993; Cui & Delage, 1996; Lloret *et al.*, 2003; Lu & Likos, 2004; Sivakumar *et al.*, 2010). Upon wetting, well-compacted fills (i.e. engineered fills) are prone to heave, whereas poorly compacted fills (i.e. un-engineered fills) are prone to settlement. Contrary to popular belief, even engineered fills can pose problems owing to substantive heave at low overburden pressures (Sivakumar *et al.*, 2010).

The deformation behaviour of unsaturated compacted clays upon wetting has been well studied within the geotechnical community. However, the impact of this deformation on buried utilities or retaining structures has received much less attention. Consider, for example, an element of compacted clay behind a retaining structure. Immediately after compaction, this element of soil is unsaturated, but subsequent rainfalls, water table fluctuations or leakage from buried utilities will increase the water content of the soil and potentially lead to saturation of the fill. This results in swelling or collapse of the fill depending on the density and state of stress within the soil. If swelling takes place under laterally restrained conditions, horizontal stresses will develop which will increase the thrust on retaining structures and potentially lead to instability (Maswoswe, 1985; Chen, 1987; Carder, 1988).

Although guidelines exist for the compaction of soil fills (*Design manual for roads and bridges*, Highways Agency, Scottish Development Department, The Welsh Office and The Department for the Environment for Northern Ireland, 1995; *Specification for highway works*, Highways Agency, Scottish Development Department, The Welsh Office and The Department for the Environment for Northern Ireland, 2004), engineers conservatively choose fill materials that can be easily analysed and that result in minimal movements during service. This choice is driven by the client demand for assets that are resilient over a long service life, for example, 120 years. Under restrained conditions, clay-based fills produce larger stresses upon wetting than granular soils (Clayton *et al.*, 1991). Symons *et al.* (1989) reported some limited information based on field studies using different types of fill material and suggested that post-compaction horizontal stresses can be as high as $0{\cdot}8 \times c_u$ in high-plasticity clay and $0{\cdot}25 \times c_u$ in low-plasticity clay (c_u is the undrained shear strength of the compacted clay). In a similar study, Mawditt (1989) reported that stresses due to saturation of compacted London Clay can be as high as 180 kPa in a retaining structure supporting 6 m of fill, with surface heave up to 140 mm.

The saturation-dependent variation of earth pressures over time in fine-grained fills is the reason why granular non-cohesive materials are generally preferred over clay. However, the use of clay fills should be promoted for two primary reasons: (*a*) sustained extraction of granular materials destroys green belts and increases the emission of carbon dioxide into the atmosphere, thus adversely impacting on the environment; (*b*) clay materials can often be sourced close to the construction site, which reduces building costs. Yet,

Manuscript received 31 January 2014; revised manuscript accepted 7 January 2015.
Discussion on this paper closes on 1 July 2015, for further details see p. ii.
* Queen's University Belfast, UK.
† ITB, Kingdom of Brunei.
‡ Université de Pau et des Pays de l'Adour, France.
§ Ulster University, UK.

practising engineers require adequate guidance about the use of compacted clay fills and on how these materials can be accommodated within current design practice.

This paper presents a laboratory-based investigation of the various factors that affect the behaviour of compacted clay fills upon restrained swelling. These factors include compaction effort, compaction water content, overburden pressure, plasticity index and mineralogy. The observed results are interpreted taking into account the impact of the bimodal pore size distribution which often exists in compacted clays (Delage *et al.*, 1996; Thom *et al.*, 2007; Monroy *et al.*, 2010; Romero *et al.*, 2011; Airò Farulla & Rosone, 2012).

EXPERIMENTAL WORK

The testing programme aims to replicate the in-situ behaviour of compacted fills wetted under laterally restrained deformation and constant overburden pressure. This corresponds, for example, to the case of a clay fill behind a retaining wall subjected to a constant post-construction load and to long-term alterations in moisture content. This type of loading conditions can be reproduced with relative ease in a modified Rowe cell for testing unsaturated soils. However, in this equipment, side friction will develop between the sample and the inner surface of the cell, particularly when testing compacted soils. Brown & Sivakumar (2008) carried out a series of tests on un-engineered and engineered compacted kaolin using a modified Rowe cell to test unsaturated soils. The cell was instrumented with pressure cells at the base and on the side wall at mid-height. The samples were saturated from the bottom. Fig. 1 shows the average vertical pressure at mid-height (the average of the pressure applied at the top and measured at the base) for a given overburden pressure applied to the top. The diagram confirms that the average pressure at mid-height was not constant (owing to significant variation of vertical pressure measured at the base close to the wetting front) during wetting. This complicated the assessment of the coefficient of earth pressure at rest (K_0). The reasons for such variations of vertical pressure are discussed in Brown & Sivakumar (2008). Based on these results, in the present investigation it was decided that a more accurate option would be the use of a stress path cell. The testing system employed in this research is the same as the one used by Boyd & Sivakumar (2011). These authors gave a complete description of sampling and testing procedures, so only a summary is presented here.

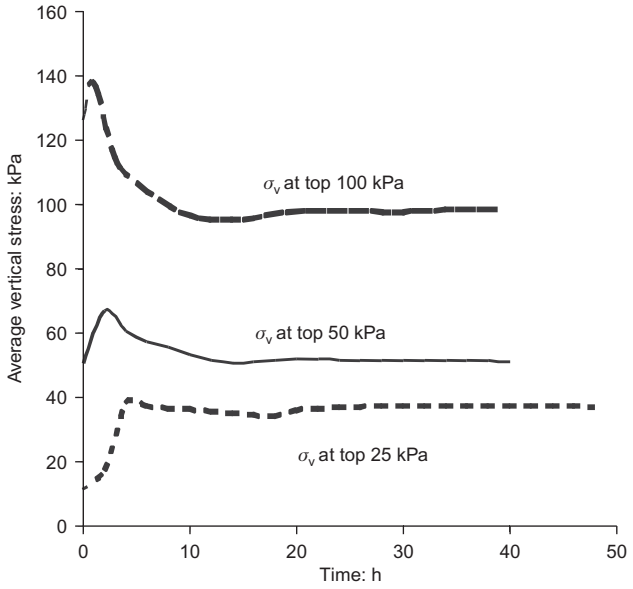

Fig. 1. Wetting of compacted kaolin in Rowe cell under various vertical pressures

Sampling

Four different materials were used in the present research, namely commercial kaolin clay (KC) supplied by WhitChem Ltd, UK, and three natural clays that have been or could be used for backfilling (Mawditt, 1989), namely London Clay (LC), Ampthill Clay (AMT) and Belfast Upper Boulder Clay (BC). The physical characteristics, plasticity classification and mineralogy of these clays are presented in Table 1. LC has the lowest percentage of clay size particles, yet is classified as a very high-plasticity clay as is AMT. KC is high plasticity and BC is classified as an intermediate to high-plasticity clay. KC and BC are non-expansive whereas LC and AMT contain a very small amount of expansive minerals. AMT clay also contains about 6% organic content.

Natural soils are deposited under one-dimensional loading conditions. However, when the soil is excavated and recompacted to form different landscapes, the loading process might no longer be one-dimensional. This is because fills are typically compacted by means of wheels or rollers that have finite horizontal dimensions. There is limited information available in the literature regarding the degree of anisotropy of compacted fills. Any attempt to prepare compacted samples in the laboratory with the same characteristics as in the field will involve significant uncertainties and will complicate the interpretation of test results. For that reason, in this work, specimens were isotropically compacted, which ensured isotropic material properties prior to wetting under laterally restrained conditions.

Tests were undertaken in a stress path apparatus on cylindrical specimens 50 mm in diameter and 50 mm high, prepared using the following procedure as suggested by Boyd & Sivakumar (2011). The three natural soils (LC, BC and AMT) were dried at 80°C, crushed and passed through a 425 μm sieve (kaolin was already available in powder form). The dry powders of the four clays were mixed with water at a target moisture content (relative to the Proctor optimum), before being sieved through a 1·18 mm aperture mesh. A rubber membrane was then placed around the 100 mm dia. pedestal of a standard triaxial cell and sealed at the base using two 'O'-rings. A stretcher was placed around the membrane and the top of the membrane was folded around the top of the stretcher. A 100 mm dia. dry porous filter was placed on the pedestal and the mixed sieved material was filled slowly into the membrane, until a height of 150 mm was achieved. Thereafter, another dry porous filter was placed above the material, followed by the top cap against which the membrane was sealed by 'O'-rings. The purpose of the dry filters was to allow drainage of air (and water, if any) from the top and bottom of the sample during compaction. The cell was assembled and the required cell pressure (based on the target dry density as explained later) was applied and maintained for 3 days while allowing pore air/water drainage. The isotropically compacted sample was then dismantled and a specimen 50 mm in diameter and 50 mm high was extruded using a thin-walled sampler.

Specimens were prepared at different water contents and compaction pressures. Table 2 lists the compression pressures, water contents and initial suctions (i.e. suctions measured after compaction by using a psychrometer) for the different materials. For each material type, one or more specimens were prepared and details of the initial conditions are given in Table 3. Ten KC specimens were prepared for the main testing programme and their initial dry densities and water contents are shown in Fig. 2 together with the

Table 1. Physical characteristics of clays

Clay type	Clay minerals	Percentage clay size fraction: %	Liquid limit: %	Plastic limit: %	Plasticity index: %	Optimum moisture content: %
Kaolin clay (KC)	Kaolinite (96·5%) Muscovite (2·2%) Quartz (1·4%)	80	70	31	39	30
London Clay (LC)	Feldspar (2%) Illite (22·5%) Kaolinite (7·1%) Montmorillonite (2·3%) Chlorite (5·4%) Quartz (49·7%) Smectite (3·1%)	40	71	27	44	23
Belfast Clay (BC)	Quartz (22·0%) Dolomite (12·7%) Muscovite (28·3%) Chlorite (8·7%) Calcite (4·1%) Kaolinite (12·1%) Montmorillonite (2%)	58	55	23	32	24
Ampthill Clay (AM)	Quartz (40·5%) Pyrite (2·5%) Muscovite (31·5%) Chlorite (5·5%) Calcite (3·5%) Feldspar (1·5%) Kaolinite (15·1%)	57	77	30	47	29

Table 2. Isotropic compaction pressures and suctions after compaction

Clay type	Fill name	Compaction water content: %	Compaction pressure: kPa	Suction: kPa
KC	Poorly engineered	25 (KC5)	800	1379
	Engineered	22 (KC12)	1200	1440
		25 (KC7, 8, 9, 15, 16)		1294
		28 (KC13)		1088
	Heavily engineered	25(KC11)	1600	1268
LC	Heavily engineered	15 (LC1)	1200	1593
		18(LC3)		1306
BC	Heavily engineered	17 (BC1)	1200	1926
		20(BC2)		1308
AMT	Heavily engineered	22(AC1)	1200	1527
		25(AC2)		1015

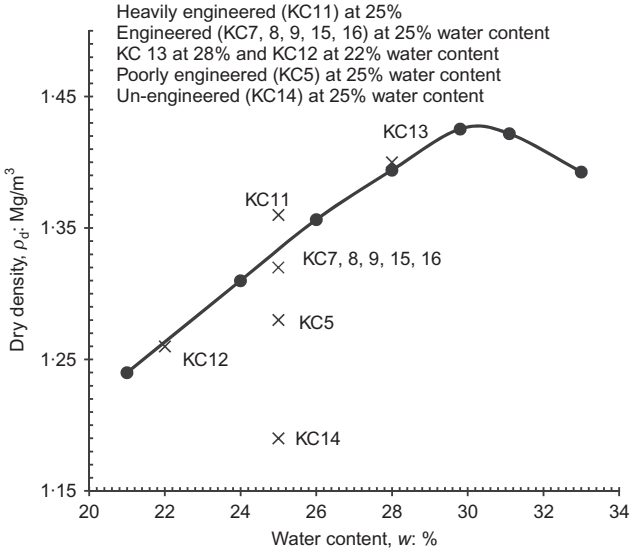

Fig. 2. Proctor compaction curve: kaolin clay

standard Proctor compaction curve. The classification of specimens in heavily engineered, engineered, poorly engineered or un-engineered (Table 2) reflects the initial state of the specimens relative to the standard Proctor curve. Heavily engineered, engineered, poorly engineered and un-engineered specimens have dry densities that are higher, equal, lower and much lower than standard Proctor, respectively.

The static isotropic pressure required for preparing engineered KC specimens (i.e. specimens with the same densities as standard Proctor) was obtained from the pressure–density relationship of statically compacted KC at 25% water content and was found to be 1200 kPa. The pressure–density relationship was measured by isotropically compressing KC at 25% water content inside a twin-cell (Sivakumar *et al.*, 2010) where water flow into the inner cell allowed measurement of the soil volume change. The same pressure of 1200 kPa was also used for preparing samples of the other three natural clays, which resulted, however, in heavily engineered samples with considerably higher dry densities than the respective Proctor curves (Fig. 3).

Table 3. Initial characteristics of specimens

Sample	w: %	ρ_d: Mg/m^3	S_r: %	$\overline{\sigma_v}$: kPa	v	v_w	Testing method
Kaolin clay (KC)							
KC5	25	1·25	59·8	50	2·115	1·666	Radially restrained
KC7	25	1·32	66·6	25	2·020	1·680	Radially restrained
KC8	25	1·32	67·5	50	2·011	1·679	Radially restrained
KC9	25	1·31	65·1	100	2·025	1·667	Radially restrained
KC11	25	1·36	70·0	50	1·942	1·659	Radially restrained
KC12	22	1·26	56·2	50	2·065	1·598	Radially restrained
KC13	28	1·40	80·6	50	1·942	1·759	Radially restrained
KC14	25	1·19	54·8	50	2·233	1·676	Radially restrained
KC15	25	1·31	65·5	100	2·030	1·674	No radial restrain
KC16	25	1·31	65·5	50	2·030	1·674	No radial restrain
London Clay (LC)							
LC1	15	1·53	66·4	50	1·586	1·389	Radially restrained
LC3	18	1·56	77·2	50	1·584	1·451	Radially restrained
Belfast Clay (BC)							
BC1	17	1·49	67·2	50	1·666	1·448	Radially restrained
BC2	20	1·62	98·4	50	1·596	1·586	Radially restrained
Ampthill Clay (AMT)							
AMT1	22	1·47	75·0	50	1·786	1·631	Radially restrained
AMT2	25	1·32	33·9	50	1·748	1·677	Radially restrained

Experimental methodology

A stress path cell was modified to allow suction control by means of the axis translation technique (Hilf, 1956). The software Triax (Toll, 1999) was used to maintain a constant net axial stress by regulating the lower chamber pressure while the cell pressure was adjusted to maintain a condition of zero radial strain throughout the wetting process. Axial and radial strains were measured using specimen-mounted inclinometers and miniature linear voltage differential transducers (LVDT), respectively. The radial strain gauge was located at mid-height of the specimen, 25 mm above the base where water drainage was permitted.

The control of radial strain was achieved through a feedback loop based on the measurement of radial deformation at the mid-height of the specimen. Initially, this posed some concerns as the deformation at mid-height might not be representative of the deformation at other heights along the specimen. Indeed the bottom of the specimen (which is closer to the water drainage) responds immediately after the start of wetting but some time will elapse before any response is observed at mid height. In order to further explore this issue some preliminary tests were performed. Fig. 4(a) presents the results from a wetting test where the suction was brought to zero in a single step from its initial value (about 1300 kPa) to zero (saturated conditions). It shows the normalised flow (i.e. the cumulative amount of water inflow to the specimen normalised by the total volume of water inflow at saturation) plotted against root time. With a standard filter (air entry value close to zero) the saturation process lasted about 10 h; however, when a 15 bar air entry value filter was used, the time increased to 140 h. This indicates that the flow through the unsaturated specimen is significantly affected by the low permeability of the high air entry filter. Such a response could be considered as 'negative' if the study was aimed at measuring the permeability of the soil. In the present case, however, it aids the uniform equalisation of water content along the specimen by slowing the wetting process. Further evidence of this is shown in Fig. 4(b), which shows the readings from two radial strain gauges located at 12·5 mm and 25 mm above the base (where water drainage is permitted). The observations show that the time lag between the responses of the two lateral strain gauges is just under 1 h. This period is considerably smaller than the duration of wetting stage of the tests carried out under laterally restrained conditions in the main testing programme. Also note that the differences in deformation at any given time are not significant. In addition, with regard to the investigation presented in Fig. 4(b), no attempt was made to measure the lateral strain at the top of the sample; however, it is expected that the difference in radial strains between the middle and top of the sample is of the same order of magnitude as the measured difference between the bottom and middle of the sample. Therefore, although the adopted experimental procedure can only enforce rigorous zero radial strain condition at the middle of the sample, it can be reasonably assumed that the measured value of the coefficient of earth pressure at rest (K_0) must not be very different from its true value that would be measured in the ideal case where a radial strain of exactly zero was maintained throughout the height of the sample.

In the event of an increase in cell pressure (to counteract lateral expansion of the specimen), a constant vertical net stress $\overline{\sigma_v}$ was maintained by reducing the lower chamber pressure, thus applying a negative deviator stress. This required a special connection on the top cap of the specimen for the application of a tensile load. Further details of experimental arrangement are detailed in Boyd & Sivakumar (2011).

The specimens were initially equalised in the triaxial cell at a suction of 400 kPa (this was the highest value of suction that could be imposed during equalisation owing to the limitations of the compressed air supply, which could attain a maximum pressure of 750 kPa). In general, the equalisation took place under an axial net stress of 50 kPa, although

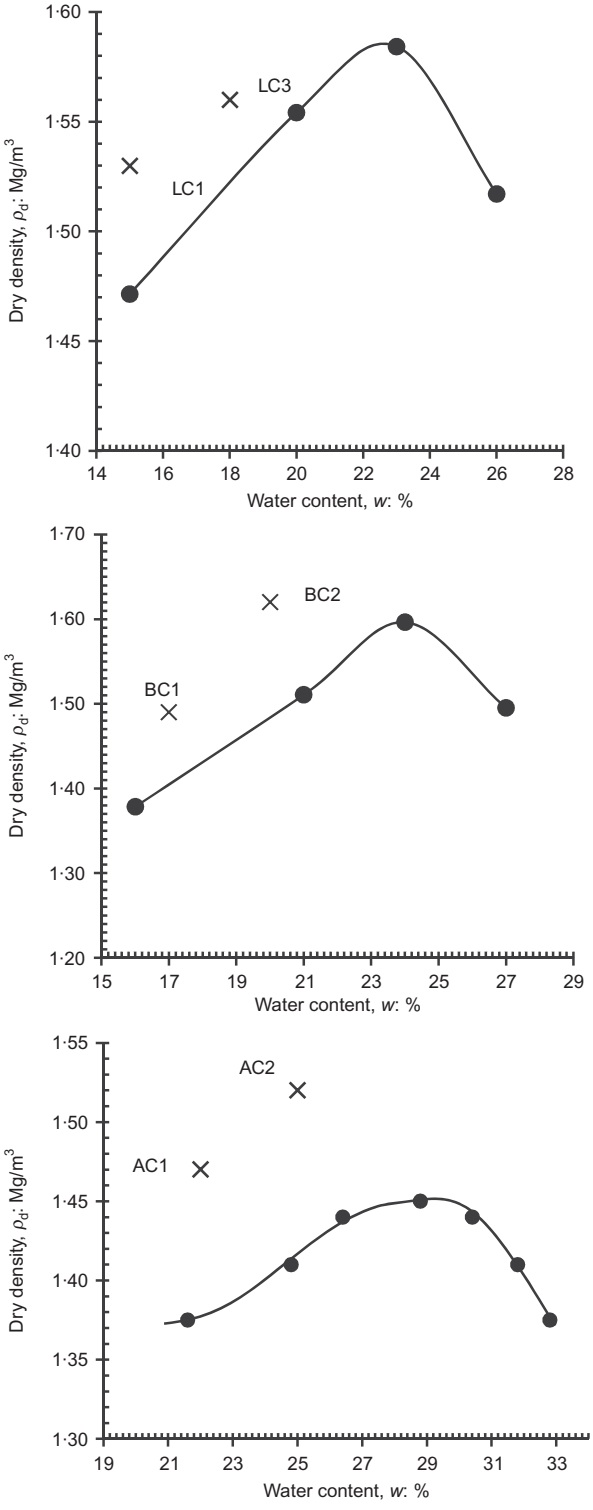

Fig. 3. Proctor compaction: London Clay, Belfast Clay and Ampthill Clay

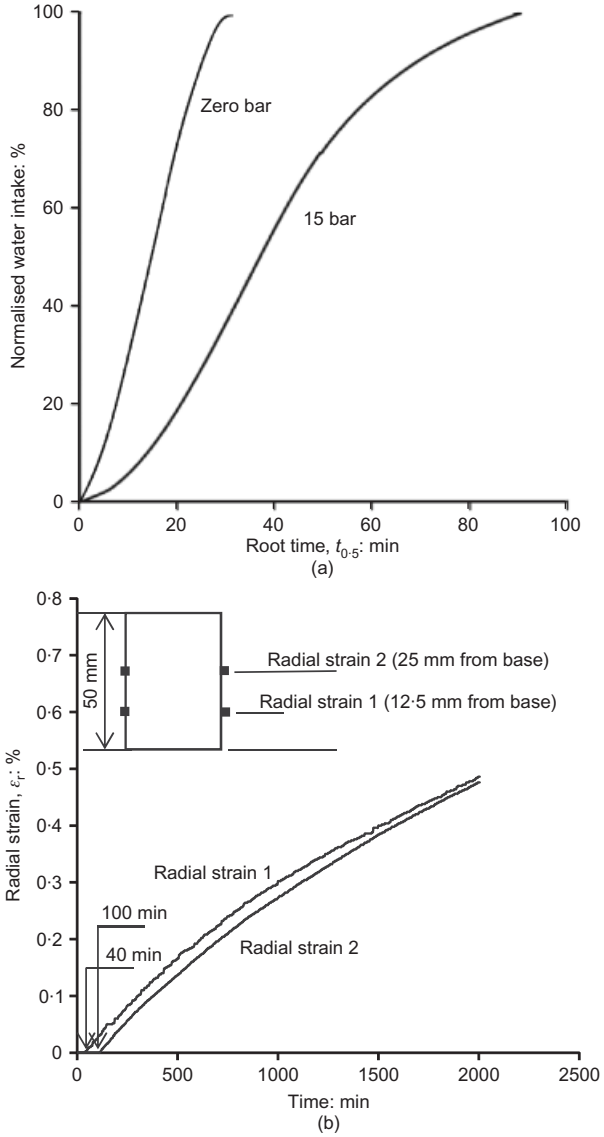

Fig. 4. Effects of ceramic filter on saturation of unsaturated soils and radial strain measurements at two locations along the height. (a) Effect of air entry ceramic filter on water flow into sample. (b) Radial strains measured at two locations along the height

the axial net stress was 25 kPa or 100 kPa in a small number of tests. Radial deformation was not restricted during the initial equalisation and therefore the radial stress was equal to the vertical stress. The equalisation stage led to an axial swelling of approximately 0·25–0·75% depending on soil type, initial water content and dry density.

Subsequently, suction was gradually reduced to zero under radially restrained conditions. Unlike Boyd & Sivakumar (2011), who wetted the specimens in a single step to a target suction value, suctions were here reduced in multiple steps of, generally, 50 kPa. The equalisation time during each step was 3–4 days for KC and 5–6 days for LC, BC and AMT. This procedure had the advantage of providing a continuous measurement of the radial net stress along the wetting path and significantly reduced fluctuations in the measurement of K_0 (a typical example of this multi-step wetting process is shown in Fig. 5). In each step, wetting was considered completed when the water flow into the specimen was less than 0·02 cm^3/day (0·05% water content). The type of tests carried out on KC and the three other natural clays are listed in Table 3.

In saturated soils, the coefficient earth pressure K_0 is defined as the ratio between horizontal and vertical effective stresses 'at rest' (no lateral straining). This definition is here extended to unsaturated soils in terms of net stresses

$$K_0^* = \frac{\sigma_h - u_a}{\sigma_v - u_a} \quad (1)$$

where σ_v, σ_h and u_a are the total vertical stress, total radial stress and pore air pressure, respectively. The symbol K_0^* is used to differentiate it from the coefficient of earth pressure of saturated soils, K_0.

Figure 6 shows the results from three preliminary tests

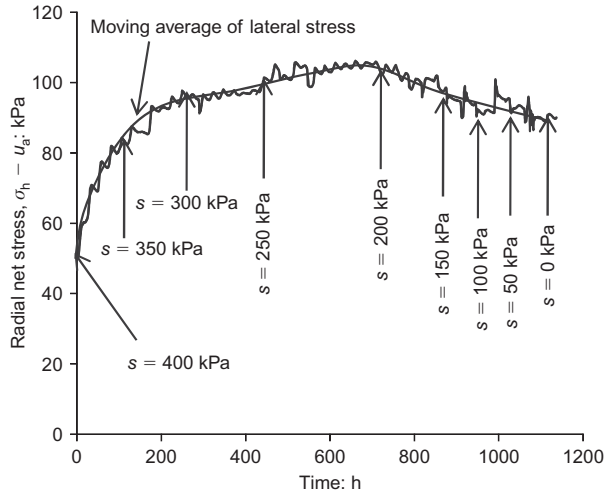

Fig. 5. Variation of radial net stress during decrease in suction by 50 kPa steps

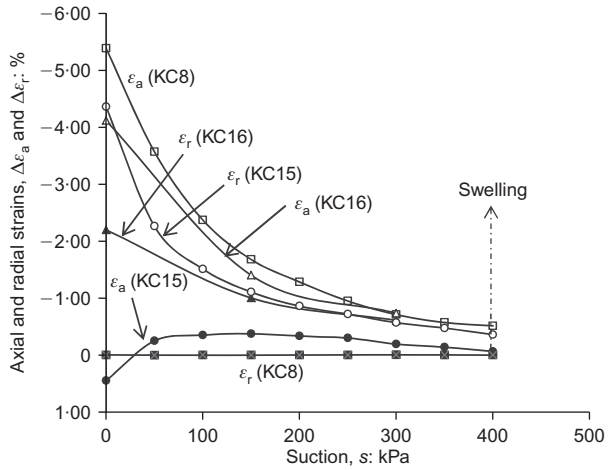

Fig. 6. Swelling/collapse of compacted kaolin

(KC8, KC15 and KC16) which were performed to explore the swelling/collapse properties of KC upon wetting with and without restriction of radial strains. The KC8 specimen, which was subjected to radially restrained conditions and a constant overburden pressure of 50 kPa, swelled axially up to 5·4%. The KC15 specimen, which was subjected to 100 kPa of axial net stress and 50 kPa of radial net stress, swelled radially by 2·6% and axially up to a maximum value of 0·3% during the first part of wetting (up to a suction of about 50 kPa), followed by collapse compression (i.e. settlement) as saturation was approached. This specimen was subjected to an anisotropic stress state, so part of the strain occurring at low suctions was caused by the soil yielding closer to critical state. At higher suctions, the sample swelled more in the radial direction than in the axial one, implying a preference for the aggregates to expand in the direction subjected to the smallest confining stress (Boyd & Sivakumar, 2011). Finally, the specimen KC16 was subjected to wetting under both axial and radial net stress of 50 kPa (i.e. isotropic stress state). The specimen swelled radially about 4·1% and axially somewhat less (2·1%) despite the fact that the fabric of the material was ostensibly isotropic.

Although this study focuses on the wetting behaviour of soils under radially restrained deformation and constant overburden pressure, a limited number of tests were also conducted to examine the behaviour during loading at constant suction. To this end, some KC specimens were wetted to suctions of zero, 150 kPa and 300 kPa under radially restrained conditions and subsequently loaded at constant suction still under radially restrained conditions. Other KC specimens were initially wetted to target suctions of 300 kPa, 150 kPa and zero without any restriction on lateral strain and subsequently taken through stress paths with $\Delta q/\Delta\bar{p} = 0$ (isotropic), $\Delta q/\Delta\bar{p} = -3/2$ and $\Delta q/\Delta\bar{p} = -\infty$, where q and $\bar{p}$ are the deviator and mean net stress respectively. The relevant test numbers are listed in Table 4. These additional tests were used to interpret soil behaviour in terms of the constitutive framework proposed by Sivakumar *et al.* (2010).

RESULTS AND DISCUSSION

The results of the wetting tests under radially restrained conditions are here discussed according to the following headings:

- effect of compaction water content (studied on KC)
- effect of compaction effort (studied on KC)
- effect of overburden pressure (studied on KC)
- effect of clay mineralogy (studied on KC, LC, BC and AMT).

A brief summary of the effects of material fabric on volume change behaviour is first given here in order to aid the discussions later. Compacted clays possess a bimodal pore size distribution (Delage *et al.*, 1996; Thom *et al.*, 2007; Monroy *et al.*, 2010; Romero *et al.*, 2011; Airò Farulla & Rosone, 2012). At small (micro) scale the individual clay particles form aggregates which are held together by suction while, at the larger (macro) scale, these aggregates are assembled to create a higher porous structure. The wetting-induced change of pore volume inside and between aggregates produces swelling or collapse of the unsaturated soil. Wetting of compacted clays will result in two different volumetric responses: swelling of aggregates and collapse

Table 4. Stress path and K_0^* loading tests at different suctions

Sample	w: %	ρ_d: Mg/m^3	Suction: kPa	Loading path
KC17	25	1·31	0	Isotropic compression*
KC18	25	1·30	0	$\Delta q/\Delta\bar{p} = -\infty$ *
KC19	25	1·29	0	K_0^* loading†
KC20	25	1·30	150	Isotropic compression*
KC21	25	1·25	150	$\Delta q/\Delta\bar{p} = -3/2$*
KC22	25	1·26	150	K_0^* loading†
KC23	25	1·32	300	Isotropic compression*
KC24	25	1·32	300	$\Delta q/\Delta\bar{p} = -3/2$*
KC25	25	1·32	300	K_0^* loading†

* Specimens were equalised to the target suction without restraining radial strains.
† Specimens were equalised to the target suction under radially restrained conditions.

compression due to aggregate slippage (Sivakumar *et al.*, 2010). The overall volumetric response is determined by which of the above two forms of behaviour is the predominant one. Thom *et al.* (2007), Romero *et al.* (2011) and Airò Farulla & Rosone (2012) presented evidence that, in a poorly compacted fill subjected to wetting at low overburden pressures, the clay aggregates expand into the inter-aggregate voids, therefore, reducing the overall volume. Conversely, in a heavily compacted fill, owing to the lack of inter-aggregate volume, any wetting-induced expansion of the aggregates translates directly into overall swelling. Monroy *et al.* (2010) presented conclusive evidence that wetting of compacted LC to saturation (zero suction) generally eradicates the bimodal pore size distribution, with a large part of the change in soil fabric taking place between suctions of 40 kPa to zero.

Effects of compaction water content (KC)

Three tests were conducted on engineered KC specimens compacted at water contents of 8% (KC12), 5% (KC8) and 2% (KC13) drier than the optimum value of 30%. Fig. 7(a) shows the increase in specific water volume against suction for these specimens. The initial values of specific water volume were 1·598, 1·679 and 1·759 for KC12, KC8 and KC13, respectively (Table 3) while the increases of specific water volume at saturation (i.e. for suction equal to zero) were 0·531, 0·394 and 0·241. The starting point of each curve corresponds to the amount of water intake during the initial equalisation stage at a suction of 400 kPa. It should be noted that intake of water during saturation increases with reducing water content at compaction. Therefore, a larger water intake should have been observed for specimen KC12 prepared at 22% water content in comparison with specimens KC8 and KC13 prepared at 25% and 28% water content, respectively. This, however, is only true below the suction of 200 kPa, whereas during the early stage of wetting, that is, between suctions of 400 and 200 kPa, the water intake of specimen KC12 appears very small. This may have been caused by the loss of water continuity between specimen KC12 and the ceramic filter, which may have also affected other aspects of the specimen responses such as the development of radial stresses and axial swelling.

Figure 7(b) shows the change in radial net stresses against suction caused by the imposition of zero radial strains. The stress increased at the start of wetting, implying that the specimens tended to expand radially. The rate of increase in radial net stress is considerable in the case of specimen KC13, which was prepared at a water content of 28% and moderate in the case of specimen KC8, which was prepared at a water content of 25%. The initial dry density of KC13 is 6% higher than that of KC8, suggesting that KC8 would have had larger macro voids into which the aggregates could expand upon wetting (Thom *et al.* (2007)). As explained earlier, the specimen KC12 prepared at 22% water content might have experienced a loss of hydraulic contact with the ceramic filter at high suction values and this is also reflected in the measurements of radial stresses. The reduced intake of water by the specimen implies that the actual suction in the specimen was higher than the target suction and consequently the specimen was much stiffer during the early stages of wetting, that is, between 400 and 200 kPa (Fig. 7(c)). Therefore any radial deformation of the specimen would have triggered significant increase in radial stress. This explains why the radial stress–suction curve for $w = 22\%$ lies above that for 25% between the suction values of 200 and 400 kPa. The trend observed below 200 kPa of suction appears consistent for all three specimens. For all specimens, the radial net stress increased upon wetting and attained a maximum value at an intermediate level of suction followed by a reduction to about 90 kPa upon saturation. The above observations can be re-interpreted in terms of K_0^* (note that the axial net stress was constant at 50 kPa) and a summary of the values of K_0^* measured in all tests is given in Table 5.

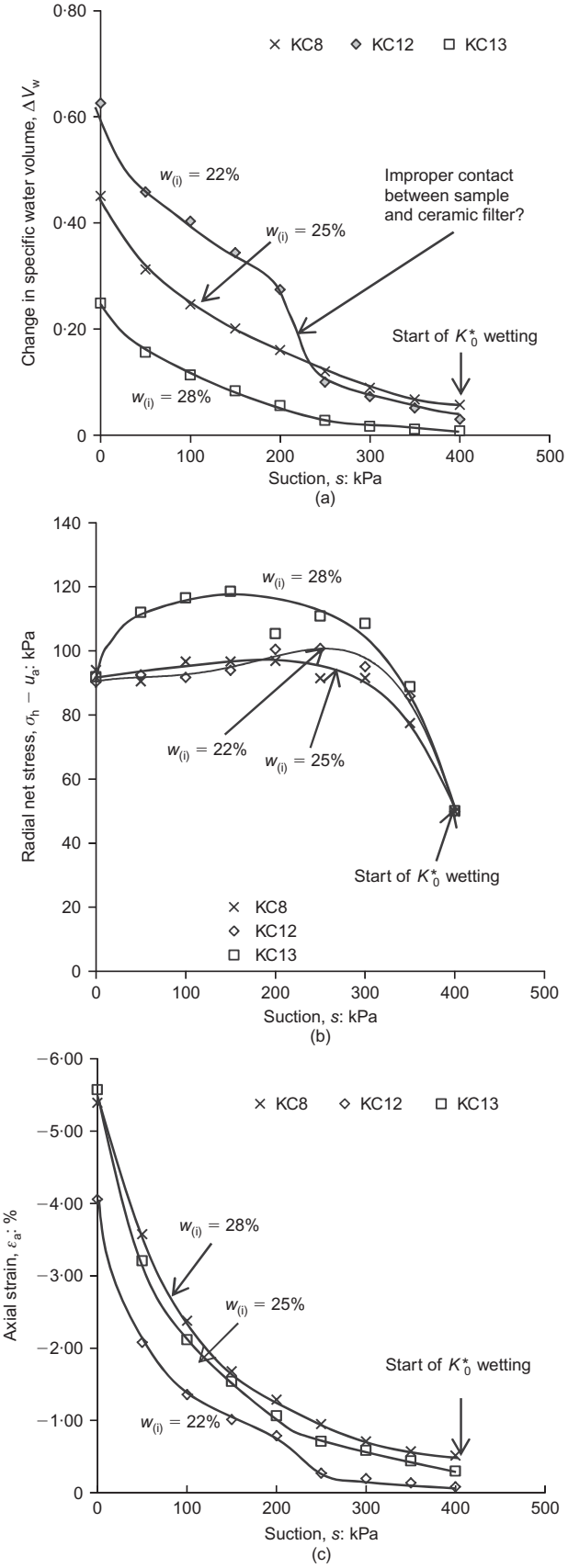

Fig. 7. Effect of compaction water content on water intake, radial net stress and axial swelling during K_0^* wetting (KC): (a) water intake; (b) lateral pressure; (c) axial expansion

Table 5. K_0^* values upon wetting

Sample	w: %	ρ_d: Mg/cm^3	$\overline{\sigma_v}$: kPa	v_w	Maximum K_0^*: suction kPa	Saturation K_0^*
KC						
KC5	25	1·25	50	1·666	1·82 (200–300)	1·60
KC7	25	1·32	25	1·680	3·60 (200)	2·80
KC8	25	1·32	50	1·679	1·97 (100–200)	1·80
KC9	25	1·31	100	1·667	1·44 (0–200)	1·42
KC11	25	1·36	50	1·659	2·74 (200–250)	2·20
KC12	22	1·26	50	1·598	2·00 (200–250)	1·80
KC13	28	1·40	50	1·759	2·40 (150–200)	2·00
KC14	25	1·19	50	1·676	1·38 (250–300)	1·14
LC						
LC1	15	1·53	50	1·389	3·30 (100–200)	2·50
LC3	18	1·56	50	1·451	3·60 (100–200)	3·42
BC						
BC1	17	1·49	50	1·448	2·60 (150)	
BC2	20	1·62	50	1·586	3·16 (150)	
AMT						
AMT1	22	1·47	50	1·631	3·50 (150–200)	2·8
AMT2	25	1·32	50	1·677	4·20 (100–150)	3·5

Figure 7(c) shows the axial strain plotted against suction for specimens KC12, KC8 and KC13. The starting point of each curve corresponds to the axial swelling undergone by the specimen during the initial equalisation stage at a suction of 400 kPa (recall that for specimen K12 a loss of contact between the soil and the ceramic filter might have occurred during the initial stages of wetting). Therefore the axial swelling at the end of equalisation was 0·1% for KC12 and increased to 0·3% and 0·6% for KC13 and KC8, respectively. Specimens KC8 and KC13 swelled by similar magnitudes during wetting under radially restrained deformation and the axial strain at saturation was about 5·4% in both cases. In the case of KC12, the axial swelling was less (~4·0%). Dry density of KC13 was higher than KC8, implying that KC13 could swell more than KC8 due to lack of inter-aggregate voids. A counteracting factor is that the initial suction in KC13 was much lower than that of KC8. In addition, KC13 experienced much higher lateral stresses than KC8. These combined effects have resulted in similar amounts of axial swelling for KC13 and KC8 upon saturation.

The above comparisons refer to three specimens compacted at similar levels of effort as the standard Proctor but different water contents. However, the initial dry density of these three specimens increases with increasing values of compaction water content. In order to investigate the effect of compaction water content at constant dry density, a comparison is made between tests KC5 and KC12, where the initial dry densities are reasonably similar but the compaction water contents are 22% and 25%, respectively. Fig. 8 shows that the radial stresses (or the value of K_0^*) developed upon wetting tend to be higher as the compaction water content is reduced for a given initial dry density. This is because drier fills have higher values of initial suctions (Table 2) and, accordingly, a higher tendency to swell upon wetting.

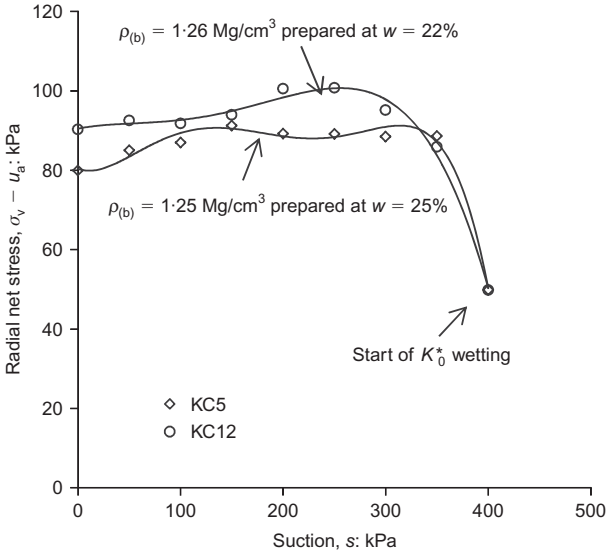

Fig. 8. Effect of compaction water content for a given initial dry density

Effects of compaction effort (kaolin clay)

The swelling potential of clay fills upon wetting is significantly influenced by compaction energy (Schanz & Tripathy, 2009; Sivakumar *et al.*, 2010). For example, heavily engineered fills exhibit larger swelling than un-engineered fills even if compacted at the same water content, which has in turn an influence on the radial pressures generated under radially restrained conditions. This aspect was examined in this work by performing wetting tests on four KC samples compacted at the same water content (25%) but under variable overburden pressures. The four specimens have different initial dry densities of 1·19 Mg/cm^3 (KC14), 1·25 Mg/cm^3 (KC5), 1·32 Mg/cm^3 (KC8) and 1·36 Mg/cm^3 (KC11) and are here categorised as: un-engineered, poorly engineered, engineered and heavily engineered. The initial suctions measured after sampling are listed in Table 2. Although specimens were compacted at the same water

content (i.e. 25%), suction tends to reduce with increasing compaction effort.

During wetting, the specific water volume increased by 0·365, 0·406, 0·451 and 0·380 for samples KC14, KC5, KC8 and KC11, respectively (Fig. 9(a)). Fig. 9(b) shows that, for all samples, the radial net stress increased up to a maximum value between suctions of 200 kPa and 300 kPa (except for sample KC8 which attained a maximum value of radial net stress for a suction between 100 kPa and 200 kPa) before reducing as the soil approached saturation. In the case of the un-engineered specimen KC14, the radial net stress slowly increased to a maximum of 69 kPa before falling to 57 kPa at full saturation. For the poorly engineered specimen KC5, the radial net stress increased to a maximum of 91 kPa before reducing to 80 kPa. Finally, in the case of the engineered and heavily engineered specimens KC8 and KC11, the maximum radial net stresses were 97 kPa and 137 kPa, respectively, while the radial net stresses at saturation were 90 kPa and 110 kPa. The corresponding maximum values of the coefficient, K_0^*, are listed in Table 5. During wetting, all specimens swelled axially by different amounts (Fig. 9(c)). The magnitude of swelling was about 0·5% axial strain for the un-engineered specimen KC14 and was as high as 6·7% for the heavily engineered specimen KC11. The observed behaviour is therefore consistent with the postulation of volumetric behaviour of compacted clays possessing a bimodal pore size distribution, as discussed earlier.

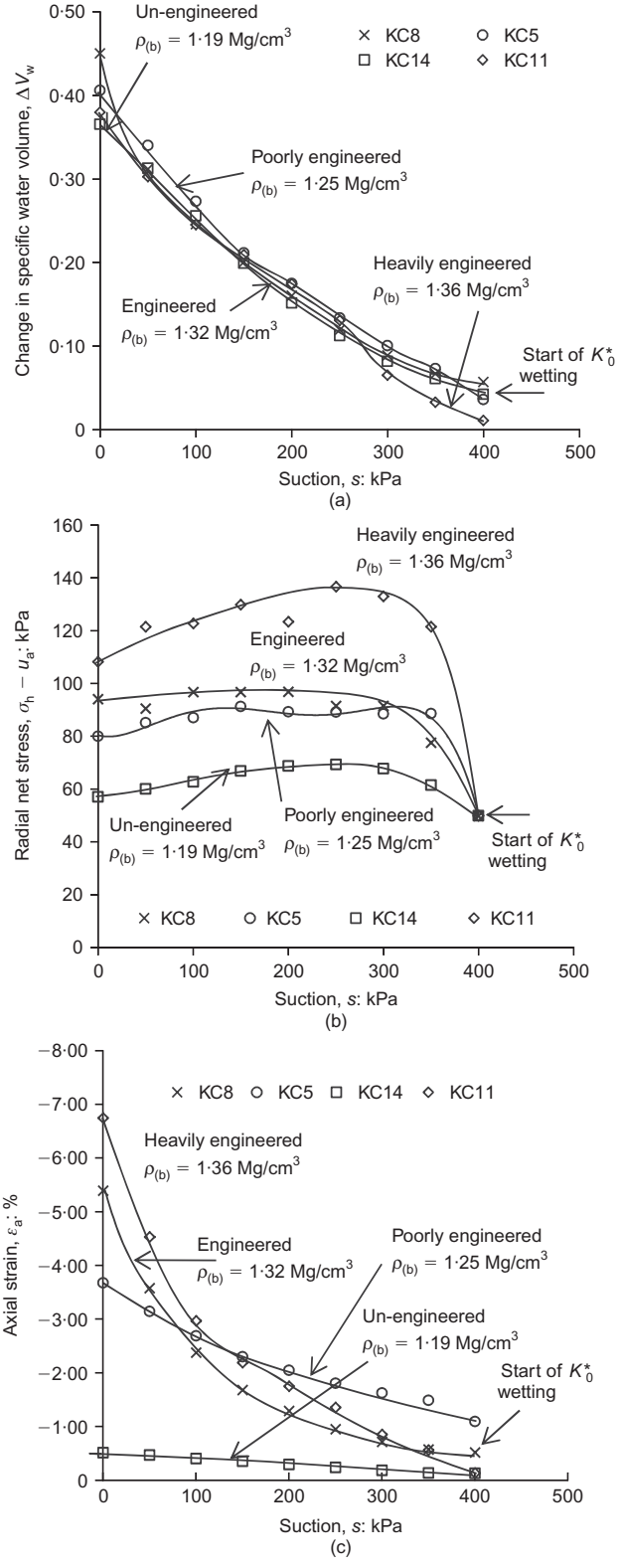

Fig. 9. Effect of initial dry density on water intake, radial net stress and axial swelling during K_0^* wetting (KC): (a) water intake; (b) lateral pressure; (c) axial expansion

Effects of overburden pressure (kaolin clay)

Three engineered specimens (KC7, KC8 and KC9) were compacted at a water content of 25% and a dry density of about 1·32 Mg/cm^3. Similarly to previous tests, the specimens underwent wetting from a suction of 400 kPa under radially restrained conditions but, in this case, they were subjected to axial net stresses of different magnitudes equal to 25 kPa, 50 kPa and 100 kPa for KC7, KC8 and KC9, respectively, to represent various depths of fill behind retaining structures. In the case of KC9, the suction was reduced from 400 kPa to 300 kPa in a single step and then by 50 kPa steps until complete saturation.

Figure 10(a) shows the measured values of radial net stress against suction for all three specimens. For specimens KC7 and KC8, the maximum radial net stresses of 90 kPa and 97 kPa, respectively, were attained at suctions between 100 kPa and 200 kPa whereas, for specimen KC9, the maximum horizontal net stress of 145 kPa was attained close to zero suction (i.e. close to saturation). Upon full saturation, the horizontal net stresses reduced to 71 kPa, 94 kPa and 141 kPa for specimens KC7, KC8 and KC9, respectively. Fig. 10(b) shows that the coefficient K_0^* reached a maximum of 3·60 in the case of specimen KC7, which was subjected to an overburden pressure of 25 kPa (corresponding to a relatively shallow depth of the fill). The relevant values of K_0^* are listed in Table 5.

Effects of clay mineralogy

Additional tests were conducted on three natural clays, namely, London Clay (LC), Belfast Clay (BC) and Ampthill Clay (AMT). For each clay type, two heavily engineered specimens were compacted at two water contents; these were 15% and 18% for LC, 17% and 20% for BC and 22% and 25% for AMT (Table 3). LC, BC and AMT are natural materials with different index properties and Proctor optimum water contents of 23%, 24% and 29% respectively. Therefore, the differences between compaction water contents and optimum water contents were relatively similar to those for KC.

London Clay: The suctions measured after sampling were 1593 kPa for sample LC1 compacted at a water content of 15% and 1306 kPa for sample LC3 compacted at a water content of 18%. Fig. 11(a) shows the water intake during wetting while Fig. 11(b) shows the corresponding change of radial net stress. For both samples, the radial net stress increased rapidly at the beginning of wetting and attained the maximum value for suctions between 100 kPa and

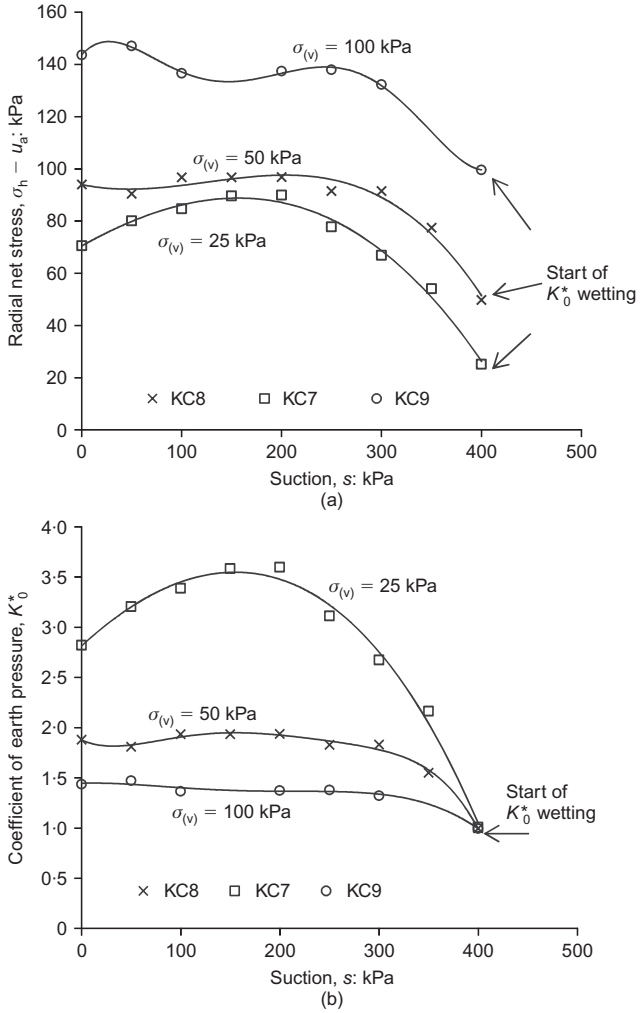

Fig. 10. Effect of overburden pressure on radial net stress and axial swelling during K_0^* wetting (KC): (a) lateral pressure; (b) K_0^*

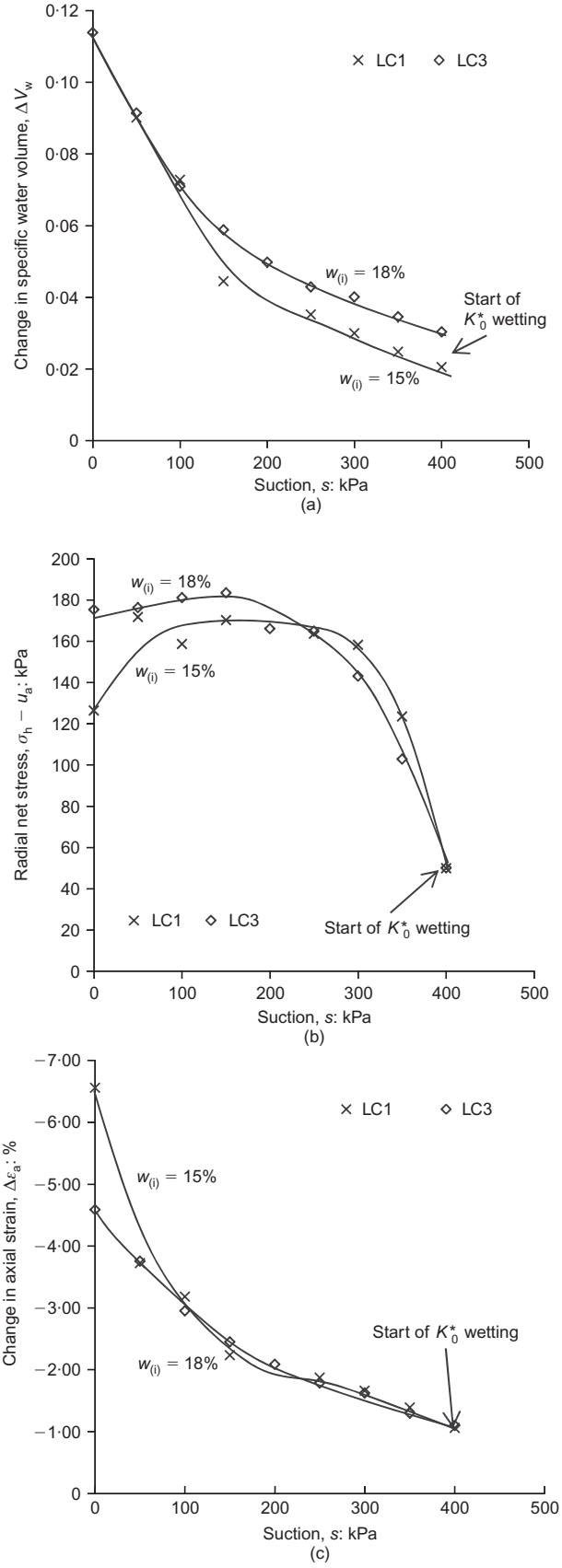

Fig. 11. Effect of compaction water content on water intake, radial net stress and axial swelling during K_0^* wetting (LC): (a) water intake; (b) lateral pressure; (c) axial expansion

200 kPa (Fig. 11(b)). In the case of the drier sample LC1, the attainment of full saturation resulted in a relaxation of the radial net stresses. The same was not true for the wetter sample LC3 (compacted at water content close to optimum), which instead experienced only a small reduction in horizontal net stress as saturation approached. The observed behaviour is in general agreement with the full-scale study reported by Mawditt (1989), who reported lateral stress of as high as 180 kPa in 6 m LC fill. The corresponding values of the coefficient K_0^* are listed in Table 5. Contrary to KC, the drier specimen LC1 experienced a higher axial swelling of 6·6% upon saturation than the wetter specimen LC3, which only swelled 4·6% (Fig. 11(c)), but noting the fact KC12 (drier specimen) did have some issues related to the continuity of water phase at the beginning of wetting.

Belfast Clay: Two specimens were compacted at water contents of 17% (BC1) and 20% (BC2), which are 7% and 4% less than the optimum value. Unfortunately, due to the failure of the air pressure supply to the laboratory, these tests had to be terminated early at a suction of 150 kPa (coincidently this happened in both tests). The change in specific water volume is shown in Fig. 12(a) while the change in radial net stress is shown in Fig. 12(b). Fig. 12(b) indicates that the maximum horizontal net stress was attained in both cases around suction of 150 kPa with the corresponding values of K_0^* listed in Table 5. Axial swelling upon saturation is equal to 3·5% and 2·6% for specimens BC1 and BC2, respectively, at the suction of 150 kPa (Fig. 12(c)).

Ampthill Clay: Two specimens were compacted at water contents of 22% (AMT1) and 25% (AMT2), which are 7%

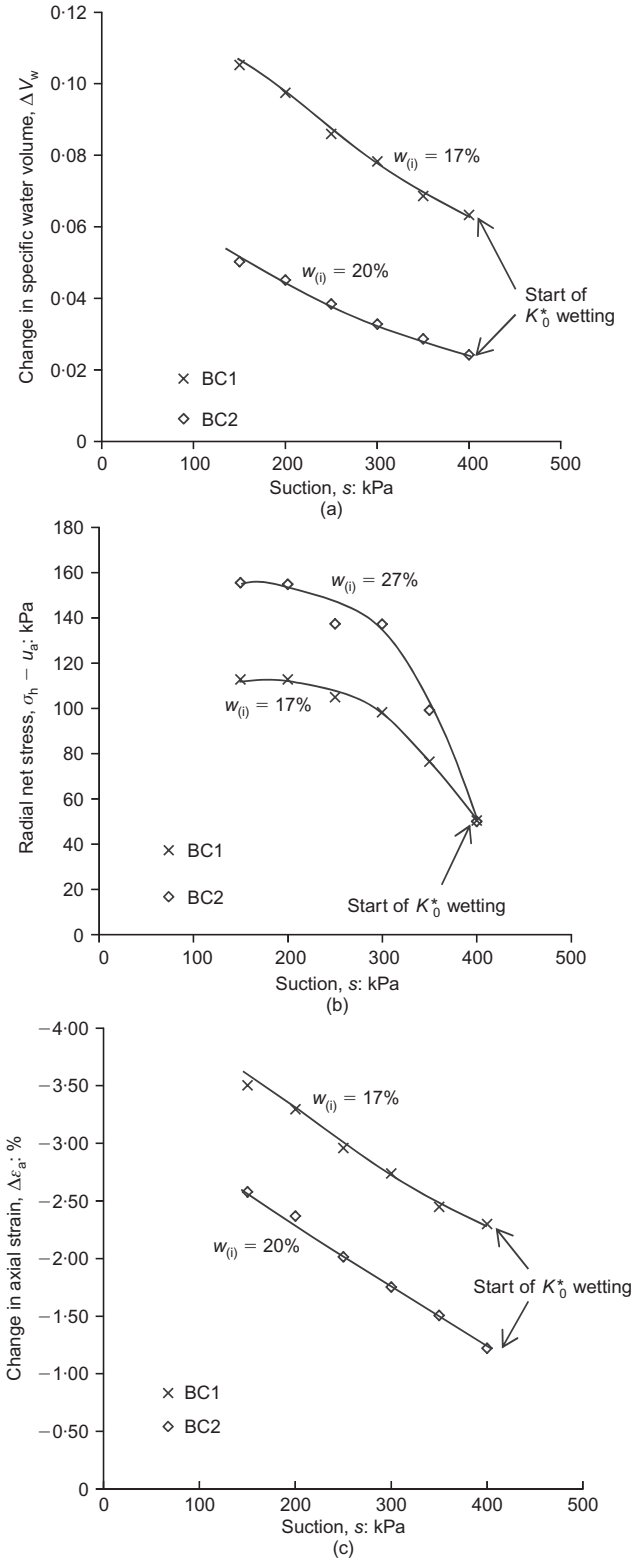

Fig. 12. Effect of compaction water content on water intake, radial net stress and axial swelling during K_0^* wetting (BC): (a) water intake; (b) lateral pressure; (c) axial expansion

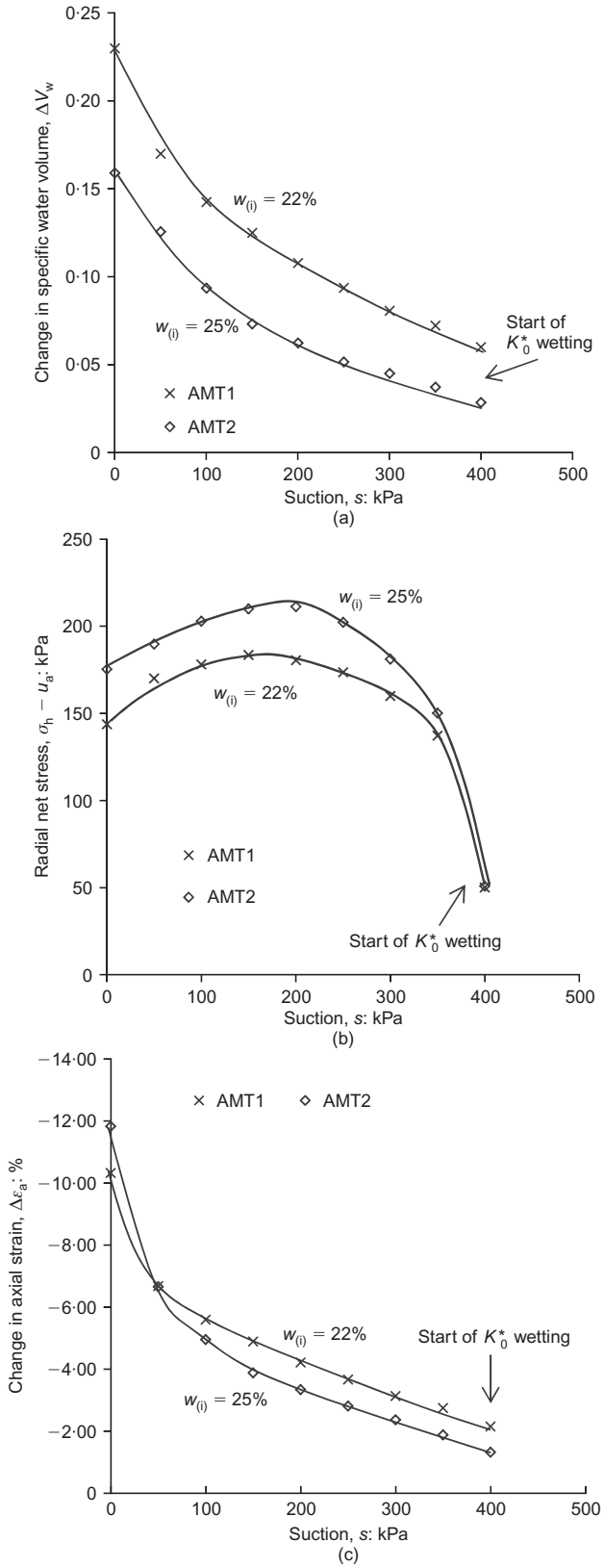

Fig. 13. Effect of compaction water content on water intake, radial net stress and axial swelling during K_0^* wetting (AMT): (a) water intake; (b) lateral pressure; (c) axial expansion

and 4% less than the optimum value. The change in specific water volume during wetting is shown in Fig. 13(a) while the corresponding change in radial net stress is shown in Fig. 13(b). The radial net stresses increased substantially at the start of wetting, attaining a maximum value for suctions between 150 kPa and 200 kPa (Fig. 13(b), but then decreased markedly upon full saturation. The corresponding values of the coefficient K_0^* are listed in Table 5. Fig. 13(c) shows that, upon saturation, the drier specimen AMT1 swelled 10·3% while the wetter specimen AMT2 swelled marginally more up to 11·8%. The magnitude of axial swelling was considerably larger for the AMT clay compared to KC, LC and BC, suggesting the presence of expansive minerals and organic materials ($\approx$ 6%) in the AMT clay.

Considering all tests, it can be deduced that in most cases a peak value of radial net stress is attained for suctions between 150 kPa and 250 kPa. After the peak, the radial net stress decreases as the soil approaches saturation but the magnitude of this reduction depends on compaction effort and overburden pressure. The differences between KC, LC, BC and AMT samples are due to variations in mineralogy, index properties, stress history and particle size distribution. The plasticity indexes of KC, LC, BC and AMT are 39%, 44%, 32% and 47%, respectively. Therefore, upon wetting, AMT and LC are expected to show larger axial swelling and greater build-up of stresses under laterally restrained conditions compared to BC and KC. This is because LC and AMT contain expansive minerals (Table 1), which are not present in significant quantities in KC and BC. In addition, AMT contains approximately 6% of organic material which further increases the swelling potential of this material. This hypothesis is supported by Figs 14(a) and 14(b), which compare the values of the coefficient K_0^* and the axial swelling for four samples of KC, LC, BC and AMT compacted at the same isotropic pressure of 1200 kPa and water contents of 25%, 18%, 20% and 25%, respectively. These water contents are between 4 and 5% less than the respective optimum values of each material.

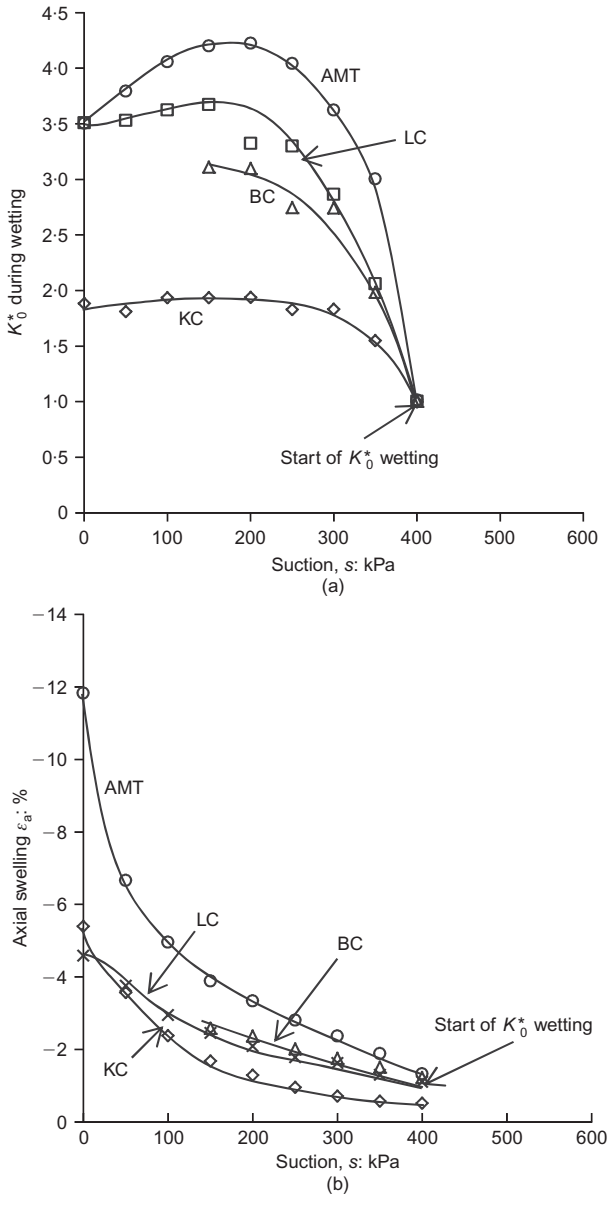

Fig. 14. Comparison of K_0^* values and axial swelling during wetting of different clays subjected to the same overburden pressure: (a) K_0; (b) axial swelling

In all tests, radial deformations were only impeded during the wetting stage, when suction was reduced from 400 kPa to zero in steps, but not during the initial equalisation stage, when suction was brought down from the relatively large value after sampling (Table 2) to 400 kPa. If radial deformation had been impeded during the entire wetting process, starting from the state after sampling, the values of the coefficient K_0^* would have probably been considerably higher than those presented here.

CONCEPTUAL MODELLING

Figure 15 shows a schematic view of the yield surface (Alonso *et al.*, 1990; Wheeler & Sivakumar, 1995; Sivakumar & Wheeler, 2000) for a compacted clay sample in the q–$\bar{p}$–s space. Upon application of the isotropic load, the stress state moves to point A on the $q = 0$ plane. The sample is then equalised at a suction of 400 kPa under a constant isotropic load with the stress state moving to point B, still on the $q = 0$ plane. At this stage, the K_0^* condition is invoked and the subsequent wetting path, that is B_{350}–B_{300}–B_{250}–B_{200}–B_{150}–B_{100}–B_{50}–B_0 (the subscript indicates the current value of suction), is followed under radially restrained deformation and constant axial net stress (the stress path is therefore contained on a plane with a $\Delta q/\Delta\bar{p}$ slope of $-3/2$). Owing to the relatively high pressures employed during compaction, the B points at higher suctions remain well within the yield locus. Therefore, the sample initially swells axially and undergoes an increase in radial net stress. As suction decreases, the radial net stress increases and this in turn increases the tensile deviator stress, taking eventually the soil on the yield locus, with the consequent occurrence of inter-aggregate slippage and plastic collapse (Thom *et al.*, 2007). There is therefore a value of suction for which the radial net stress reaches a maximum (represented by point X in Fig. 15) and, if suction decreases further, the radial net stress and the tensile deviator stress start decreasing as the soil undergoes plastic compression.

Yield domain in q–$\bar{p}$–s space

The preceding sections have examined the effect of dry density, compaction water content and overburden pressure on the build-up of radial stresses during wetting under radially restrained conditions. In order to provide a quantitative explanation of the observed behaviour, an attempt is made to establish the yield surface of KC compacted to 1200 kPa at a water content of 25%. Six specimens were wetted to suctions of zero (KC17 and KC18), 150 kPa (KC20 and KC21) and 300 kPa (KC23 and KC24) under an isotropic stress state 50 kPa and subsequently subjected to further isotropic or radial compression at constant suction (refer to Table 4 for the direction of stress path). Yield stresses were calculated by using a simple graphical construction as suggested by Casagrande (1936). These yield stresses are indicated by open circular data points in Fig. 16, together with a qualitative estimate of the constant suction yield loci, to aid interpretation of the test results presented in the next section.

Stress path loading: three specimens, KC19, KC22 and KC25, were equalised under an isotropic stress of 50 kPa (see Table 4) at suction of 400 kPa. They were then gradually wetted under radially restrained conditions and constant axial net stress (50 kPa) to target suctions of zero, 150 kPa, and 300 kPa, respectively. After this, suction was maintained constant and the axial stress was increased still under

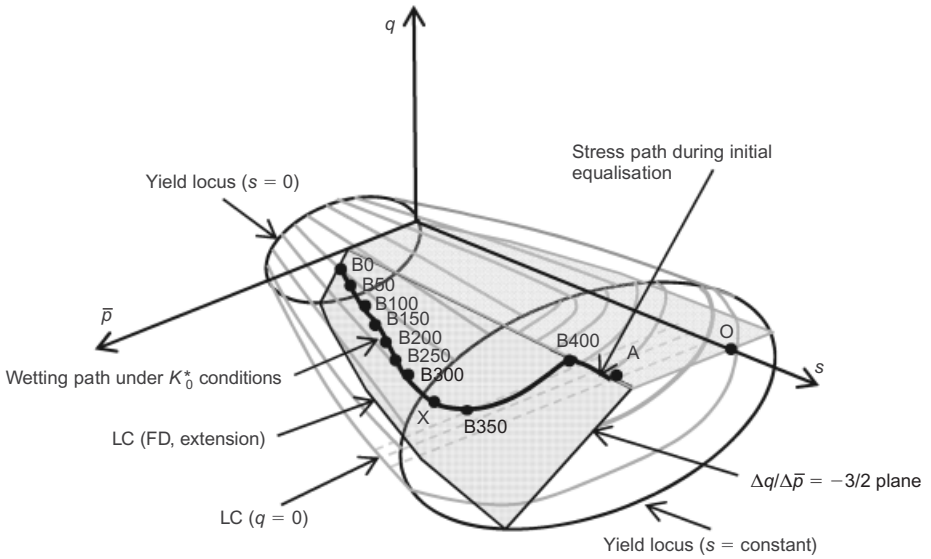

Fig. 15. Conceptual modelling and yield surface for kaolin clay

radially restrained conditions. Figs 16(a), 16(b) and 16(c) show the point corresponding to the end of wetting together with the subsequent loading in the q–$\bar{p}$ plane at suctions of zero, 150 and 300 kPa, respectively. During K_0^* wetting to suctions of 150 and 300 kPa, the stress path remained inside the initial yield boundary but, during K_0^* wetting to zero suction, the stress path crossed the initial yield locus. This implies that wetting to zero suction may have induced some plastic straining as the stress path approached saturation. In all three cases, the K_0^* wetting terminated at a negative value of deviator stress (i.e. −54 kPa, −60 kPa and −77 kPa for suction values of zero, 150 and 300 kPa, respectively) and the subsequent K_0^* loading increased the deviator stress back to positive values.

The slope of the K_0^* loading path is very steep at the start but then gradually reduces and approaches a straight line for higher values of deviator stress. At zero suction, the stress path approaches the saturated K_0^* line soon after the start of loading because the previous wetting stage had produced plastic deformation. At the other two values of suction, the behaviour is very similar to that of an over-consolidated saturated soil. Interestingly, the slopes of the K_0^* lines at different suctions are reasonably parallel, although the intercepts depend on suction and become smaller as suction reduces to zero. At a suction value of zero, one would expect the intercept to be zero, although the observed behaviour indicates that this is not true, probably because of the aggregated structure of the compacted soil even at the saturated state (Thom *et al.*, 2007).

Figure 17 shows the wetting path of specimens KC11, KC8, KC5 and KC14 (regarded as heavily engineered, engineered, un-engineered and poorly engineered) in the q–s and s–$\bar{p}$ planes. All specimens were compacted at the same water content of 25% but were subjected to different compaction efforts. The specimens were wetted under radially restrained conditions with a constant overburden pressure of 50 kPa. Also included in Fig. 17 are the yield loci for KC8 (engineered specimen). Naturally, these yield loci are only relevant to KC8 and are not applicable to KC5, KC11 and KC14, as these specimens have different initial dry densities and therefore different yield loci. As per KC8, the wetting path is initially well within the yield domain and only approaches yielding when suction is reduced to about 50 kPa (Fig. 17(b)), confirming the earlier discussion on the development of lateral stresses during wetting.

CONCLUSIONS

Compacted fills made of clay are becoming more common in construction practice. Wetting of compacted fills around buried rigid structures or behind retaining walls, can lead to the development of excessive stresses inside the soil. The magnitude of these stresses is influenced by several factors which include: dry density, overburden pressure, stress history, compaction water content and clay mineralogy. This paper has examined these factors through a body of laboratory investigations and the main conclusions are listed below.

- Compacted clay fills are unsaturated at the time of placement and the value of initial suction can vary significantly, being largely influenced by compaction water content.
- Post-compaction wetting (i.e. saturation) leads to a gradual reduction in suction under constant overburden pressure. If the deformation of the compacted material is restricted, this wetting process may cause the development of excessive stresses inside the soil. This can lead to a significant increase in K_0^* values (the ratio between horizontal net stress and vertical stress).
- Continued wetting of the specimens resulted in some relaxation of lateral stresses, particularly when approaching a near-saturated state.
- The magnitude of wetting-induced stresses (and therefore the value of K_0^*) was significantly affected by the initial dry density, compaction water content, overburden pressure, stress history and clay mineralogy. The most significant development of stress was observed in the case of Ampthill Clay which contained a certain percentage of expansive minerals and a marginal organic content.
- During laboratory tests, specimens were restrained from deforming radially, although they were allowed to deform in the axial direction. The axial expansions of the specimens were again influenced by the above-mentioned factors. In the case of Ampthill Clay, the axial expansion was significant and as high as 12%.
- The observed behaviour was explained using a conceptual constitutive model for the soil. In a limited number of tests on kaolin clay the value of K_0^* was measured under axial loading at constant suction and radially restrained deformation. Test results showed that the slope of the K_0^* line was unaffected by the suction value.

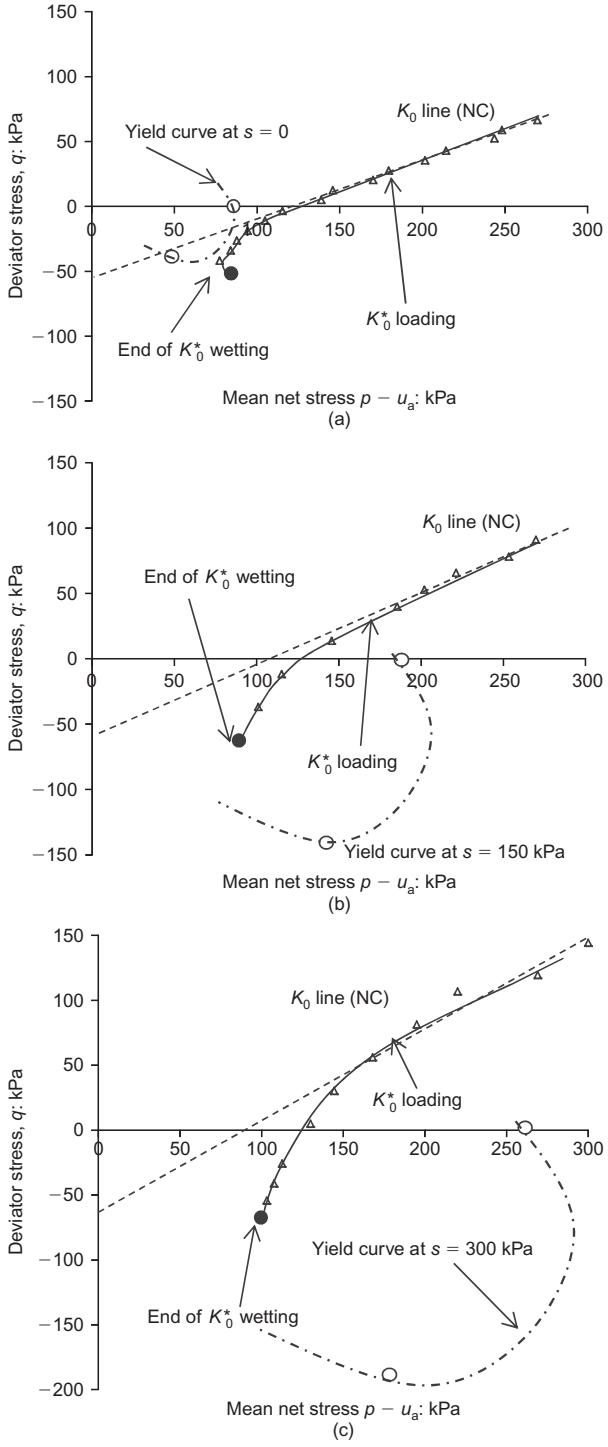

Fig. 16. Stress path during K_0^* loading and yield locus at different suctions (KC): (a) suction, $s = 0$; (b) suction, $s = 150$ kPa; (c) suction, $s = 300$ kPa

- The above conceptual model allows understanding of the response of compacted fine-grained fills to variations in overburden pressure, wetting, stress history and initial density/soil suction. This model can therefore be used by designers to understand the impact of long-term moisture changes within the fill and the associated changes of the coefficient of earth pressure at rest.

NOTATION

c_u	undrained shear strength of compacted clay
K_0	coefficient of earth pressure in saturated soil at rest
K_0^*	coefficient of earth pressure in unsaturated soil

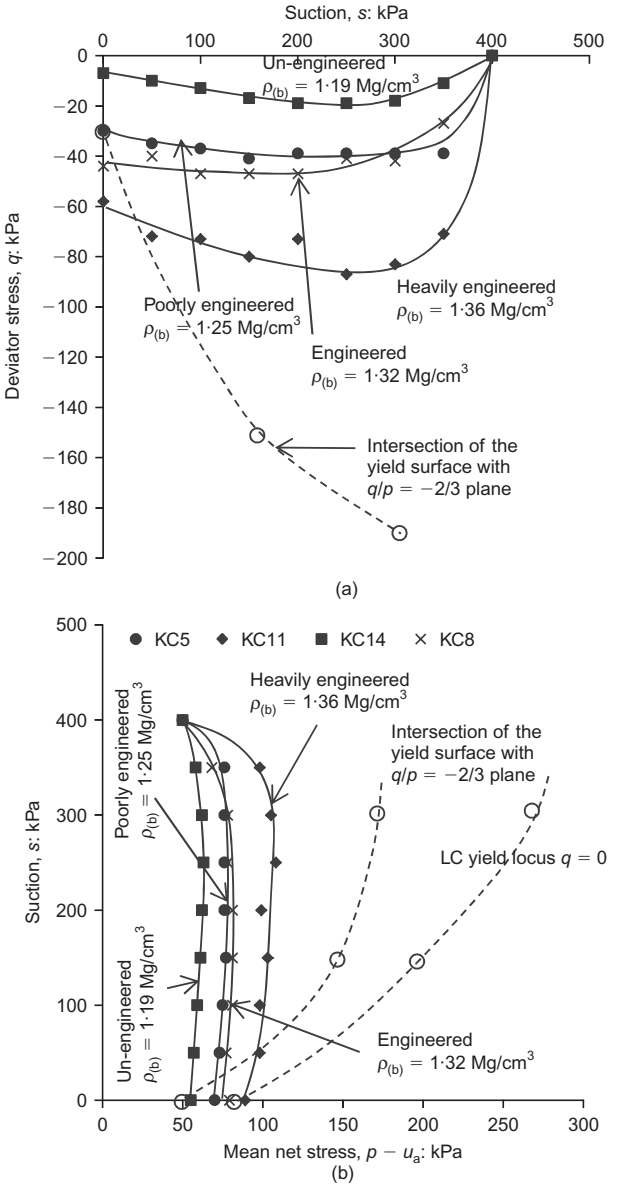

Fig. 17. Stress paths during K_0^* wetting for kaolin clay: (a) K_0^* path during wetting in q–s plane; (b) K_0^* path during wetting in p–s plane

$\bar{p}$	mean net stress
q	deviator stress
S_r	degree of saturation
s	suction
u_a	pore air pressure
v	specific volume
v_w	specific water volume
w	water content
ε_a	axial strain
ε_r	radial strain
ρ_d	dry density
σ_h	total radial stress
σ_v	total vertical stress
$\overline{\sigma_v}$	net vertical stress

REFERENCES

Airò Farulla, C. & Rosone, M. (2012). Microstructure Characteristics of Unsaturated Compacted Scaly Clay. *Proceedings of 2nd European conference on unsaturated soils (unsaturated soils: research and applications)*, Naples, Italy, pp. 123–130. Heidelberg, Germany: Springer.

Alonso, E. E., Gens, A. & Josa, A. (1990). A constitutive model

for partially saturated soils. *Géotechnique* **40**, No. 3, 405–430, http://dx.doi.org/10.1680/geot.1990.40.3.405.

Boyd, J. L. & Sivakumar, V. (2011). Experimental observations of the stress regime in unsaturated compacted clay when laterally confined. *Géotechnique* **61**, No. 4, 346–363, http://dx.doi.org/10.1680/geot.2011.61.4.345.

Brown, J. & Sivakumar, V. (2008). The changes in stress regime during wetting of unsaturated compacted clays when laterally confined. In *Unsaturated soils: advances in geo-engineering* (eds D. G. Toll, C. E. Augarde, D. Gallipoli and S. J. Wheeler), pp. 361–367. Leiden, the Netherlands: Balkema, CRC Press.

Carder, D. R. (1988). Earth pressures on retaining walls and abutments. *Ground Engng* **21**, No. 5, 7–10.

Casagrande, A. (1936). The determination of the pre-consolidation load and its practical significance. *Proceedings of the 1st international conference on soil mechanics*, Cambridge, Massachusetts, vol. 3.

Charles, J. A. (1993). *Building on fill: Geotechnical aspects*. Watford, UK: The Building Research Establishment.

Chen, F. H. (1987). Lateral expansion pressure on basement walls. *Proceedings of the 6th international conference on expansive soils, New Delhi, India* vol. 1, pp. 55–59. Boca Raton, FL, USA: CRC Press.

Clayton, C. R. I., Symons, J. C. & Hiedra, C. (1991). The pressure of clay backfill against retaining structures. *Can. Geotech. J.* **28**, No. 2, 282–297.

Cui, Y. J. & Delage, P. (1996). Yielding and plastic behaviour of an unsaturated compacted silt. *Géotechnique* **46**, No. 2, 291–311, http://dx.doi.org/10.1680/geot.1996.46.2.291.

Delage, P., Audigiuer, M., Cui, Y. J. & Howat, M. D. (1996). Microstructure of a compacted silt. *Can. Geotech. J.* **33**, No. 1, 150–158.

Highways Agency, Scottish Development Department, The Welsh Office and The Department for the Environment for Northern Ireland (1995). *Earthworks design and preparation of contract documents, HA 44/91; Design manual for roads and bridges, Geotechnical drainage*, vol. 4. London, UK: Her Majesty's Stationery Office.

Highways Agency, Scottish Development Department, The Welsh Office and The Department for the Environment for Northern Ireland (2004). *Manual of contract documents for highways works MCHW1; Specification for highways works*, Series 600. London, UK: Her Majesty's Stationery Office.

Hilf, J. N. (1956). *An investigation of pore water pressure in compacted cohesive soils*, Technical Memorandum 654. Denver, USA: U. S. Department of Interior Bureau of Reclamation.

Lloret, A., Villar, M. V., Sanchez, M., Gens, A., Pintado, X. & Alonso, E. E. (2003). Mechanical behaviour of heavily compacted bentonite under high suction changes. *Géotechnique* **53**, No. 1, 27–40, http://dx.doi.org/10.1680/geot.2003.53.1.27.

Lu, N. & Likos, W. J. (2004). *Unsaturated soil mechanics*. New York, NY, USA: Wiley.

Maswoswe, J. (1985). *Stress path for a compacted soil during collapse due to wetting*. PhD thesis, Imperial College London, London, UK.

Mawditt, J. M. (1989). Discussion: Conventional retaining walls: pilot and full-scale studies. *Proc. Instn Civ. Engrs, Part 1* **86**, No. 5, 980–986.

Monroy, R., Zdravkovic, L. & Ridley, A. (2010). Evolution of microstructure in compacted London clay during wetting and loading. *Géotechnique* **60**, No. 2, 105–119, http://dx.doi.org/10.1680/geot.8.P.125.

Romero, E., Della Vecchia, G. & Jommi, C. (2011). An insight into the water retention properties of compacted clayey soils. *Géotechnique* **61**, No. 4, 313–328, http://dx.doi.org/10.1680/geot.2011.61.4.313.

Schanz, T. & Tripathy, S. (2009). Swelling pressure of a divalent-rich bentonite: Diffuse double-layer theory revisited. *Water Resources Res*. **45**, No. 5, W00C12.

Sivakumar, V. & Wheeler, S. J. (2000). Influence of compaction procedure on the mechanical behaviour of an unsaturated compacted clay, Part 1: Wetting and isotropic compression. *Géotechnique* **50**, No. 4, 359–368, http://dx.doi.org/10.1680/geot.2000.50.4.359.

Sivakumar, V., Sivakumar, R., Murray, E. J., Mackinnnon, P. & Boyd, J. (2010). Mechanical behaviour of unsaturated kaolin (with isotropic and anisotropic stress history). Part 1: Wetting and compression behaviour. *Géotechnique* **60**, No. 8, 581–594, http://dx.doi.org/10.1680/geot.8.P.007.

Symons, I. F., Clayton, C. R. I. & Darley, P. (1989). *Earth pressure against an experimental retaining wall backfilled with heavy clays*, research report 192. Crowthorne, Berkshire, UK: Transport and Research Laboratory.

Thom, R., Sivakumar, V., Sivakumar, R., Murray, E. J. & Mackinnon, P. (2007). Technical Note: Pore size distribution of unsaturated compacted kaolin: the initial states and final states following saturation. *Géotechnique* **57**, No. 5, 469–474, http://dx.doi.org/10.1680/geot.2007.57.5.469.

Toll, D. G. (1999). A data acquisition and control system for geotechnical testing. In *Computing developments in civil and structural engineering* (eds B. Kumar and B. H. V. Topping), pp. 237–242. Edinburgh, UK: Civil-Comp Press.

Wheeler, S. J. & Sivakumar, V. (1995). An elasto-plastic critical state framework for unsaturated soil. *Géotechnique* **45**, No. 1, 35–53, http://dx.doi.org/10.1680/geot.1995.45.1.35.